Materials Science & Engineering A 634 (2015) 161–166

Contents lists available at ScienceDirect

Materials Science & Engineering A

journal homepage: www.elsevier.com/locate/msea

Grain boundary dynamics of SiC bicrystals under shear deformation

Stefan Bringuier*, Venkateswara Rao Manga, Keith Runge, Pierre Deymier, Krishna Muralidharan

University of Arizona, Department of Materials Science and Engineering, Tucson, AZ 85721, USA

ARTICLE INFO

Article history:
Received 13 January 2015
Received in revised form
4 March 2015
Accepted 5 March 2015
Available online 14 March 2015

Keywords:
Stick-slip
Athermal dislocation climb
Slide–climb
Silicon carbide
Bicrystals

ABSTRACT

The dynamics of SiC grain boundaries under shear are characterized using molecular dynamics simulations. At low-temperatures, low-angle grain boundaries exhibit stick-slip behavior due to athermal climb of edge dislocations along the grain boundary. With increasing temperature stick-slip becomes less pronounced due to dislocation glide, and at high-temperatures, structural disordering of the low-angle grain boundary inhibits stick-slip. In contrast, structural disordering of the high-angle grain boundary is induced under shear even at low temperatures, resulting in a significantly dampened stick-slip behavior.

1. Introduction

Cubic silicon carbide (3C-SiC) is an important technological material finding uses in applications such as ceramic armors, nuclear-fuel claddings, abrasives and sensors [1,2]. Consequently, there has been an ongoing effort in developing a fundamental characterization of 3C-SiC properties under thermal and mechanical stimuli [3–5]. Toward this end, using classical molecular dynamics (MD) simulations, we examine the mechanical response of 3C-SiC bicrystals consisting of symmetric tilt grain-boundaries (GBs) under shear loading and characterize the effect of temperature on the ensuing shear response. We pay special attention to the dynamics of low-angle and high-angle symmetric tilt GBs; in particular, the GBs that are examined include Σ365 and Σ25, which have a rotation axis of [001] and a (110) median boundary plane, respectively. While the energetics and structural characteristics of these symmetric tilt GBs in 3C-SiC have been documented from atomistic simulations [6], so far, there has been no concerted attempt at characterizing their dynamic response to mechanical stimulus. In this regard, the current study will provide important insights into the atomic-scale mechanisms that govern the mechanical response of the considered GBs under shear, thereby enabling a nuanced understanding of temperature dependent and stress induced plastic deformation mechanisms that are active in polycrystalline 3C-SiC.

2. Background

It is well known that GBs play a crucial role in determining the mechanical behavior of materials and in this context, MD simulations and experiments have examined GB dynamics in metallic [7–9] and ceramic [10–13] bicrystals. In metallic bicrystals, grain boundary sliding occurs via stick-slip, sometimes accompanied by temperature-dependent coupled lateral GB migration (i.e., normal motion of the GB) [8,9]. In experiments of ceramic bicrystals of zirconia and alumina, GB sliding was shown to be the predominant deformation mechanism; in particular, in zirconia bicrystals, a combination of climb and glide of dislocations was responsible for GB sliding, and for specific coincident site lattices, GB sliding was simultaneously accompanied by GB migration [12,13].

In addition, there have also been relevant studies on examining 3C-SiC GBs [4,14–18]. For example, the response of nanocrystalline 3C-SiC to indentation demonstrated a crossover from intergranular to intragranular deformation at critical indenter depths [14]. This phenomenon was attributed to cooperative GB sliding, grain rotations, and dislocation glide as well as competition between crystallization and amorphization. Furthermore, 3C-SiC symmetric twist bicrystals have been explored under mechanical loading with and without irradiation [17]. It was seen that the GB dynamics and the ensuing mechanical response of the bicrystal were critically dependent on the intensity of the irradiation dose. As a next step in furthering the understanding of SiC GBs in response to mechanical stimulus, we examine model symmetric tilt GBs under shear loading as a function of temperature.

* Corresponding author.
E-mail address: stefanb@email.arizona.edu (S. Bringuier).

http://dx.doi.org/10.1016/j.msea.2015.03.022
0921-5093/

3. Simulation methodology

The accuracy of classical MD simulations is governed by the choice of the underlying interatomic potential used for describing the interaction between constituent atoms (and molecules). While interatomic potentials are typically parameterized to replicate materials' thermodynamic properties that are either derived from first-principles or from experiment, they can provide valuable insight into the atomic-scale mechanisms that govern the mechanical response of materials to external stimuli [19,20]. Nevertheless, due precautions are needed while analyzing MD data since MD simulations tend to systematically overestimate yield and failure stress/strain when compared to experimental data. The overestimation can be attributed to the fact that the size of MD simulation cells are at best, 100s of nanometers (with or without periodic boundaries), thereby precluding the incorporation of large defects. Furthermore, MD simulations can only be carried out at high strain rates (as compared to experimentally achievable rates) due to computational constraints, and this serves as an additional reason for the systematic deviations from experiments while comparing MD and experimentally derived yield and fracture stress/strains.

In order to examine the SiC GBs under study, we use the MD simulation package LAMMPS [21], while visualization of the MD trajectories is carried out using OVITO [22]. The interatomic interactions for Si–C, Si–Si, and C–C used in this work are described by the Tersoff bond-order potential [23,24]. The Tersoff potential is composed of two- and three-body functions that properly capture the angular dependence necessary for describing covalent bonding. The energy between two atoms i and j is given by

$$V_{ij} = f_c(r_{ij})\left[f_R(r_{ij}) + f_b(r_{ij}, r_{ik}, \theta_{ijk})\, f_A(r_{ij})\right] \quad (1)$$

Here, f_R and f_A are the repulsive and attractive pairwise contributions to the interatomic potential energy, respectively, and f_c is a smooth cutoff function. The function f_b is a three-body bond-order function, which modulates the attractive term based on the local chemical environment of an atom. In this work, we make use of the Tersoff parameter set, which has been suitably modified to correctly predict the ground-state structure, energies, and elastic properties of both 3C-SiC and amorphous SiC [24]. Furthermore, it has been used to investigate the mechanical behavior under various loading conditions and irradiation (with addition of ZBL potential) of 3C-SiC [15–17,25]. The parameter set used in this work also adapts the change in Si–Si cut-off from 3.0 Å to 2.85 Å as done in Refs. [6,26] to ensure no second-nearest neighbor interactions that would otherwise occur due to small atomic distortions.

The construction of 3C-SiC symmetric tilt GBs follows the procedure outlined by Wojdyr et al. [6]. Symmetric tilt GBs with varying misorientation angles (4.24°–36.87°) are generated using the coincident site lattice model with a rotation axis of [100] and a median boundary plane (110) and contain approximately 60,000 atoms with dimensions $160 \times 160 \times 40$ Å^3. The as-constructed systems are energy-minimized by displacing the grains with respect to each other, as shown in Fig. 1(a), in increments of 0.1 Å with the displacement restricted to the GB plane. For each incremental displacement, the bicrystal is taken through an annealing step, where the simulation cell is cyclically heated and cooled, during which, the atomic positions are saved every 5 ps and each of these snapshots are subsequently minimized using the conjugate gradient method. For a given misorientation angle, the snapshot with the lowest GB energy is taken as the energy-minimum structure (see Ref. [6] for more details). We note that although it has been shown that GB composition can differ than that of the bulk 3C-SiC [26], the focus of the work presented here is on stoichiometric GBs.

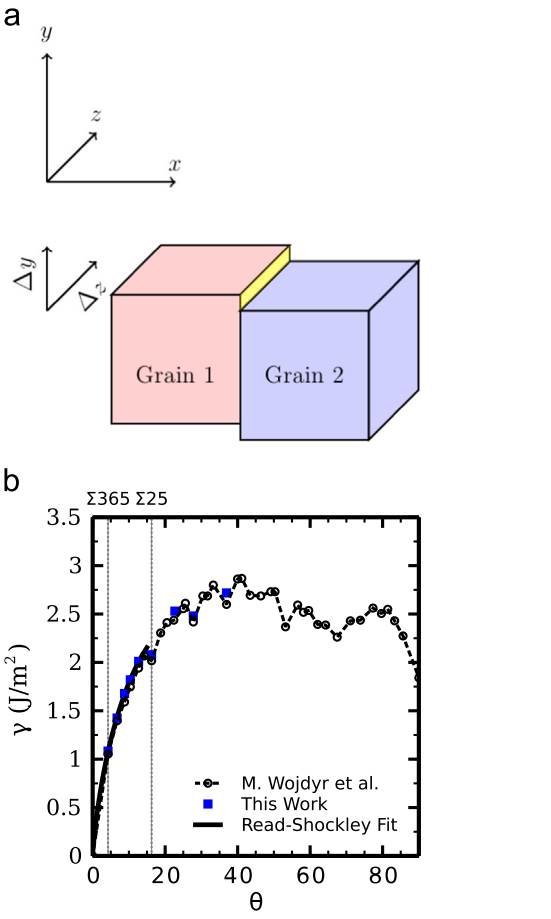

Fig. 1. (a) Schematic of incremental relative displacement of grains during energy minimization search. (b) GB energy vs. misorientation angle. Results compared to those of Wojdyr et al. [6] and are in good agreement.

As shown in Fig. 1(b) the variation in energy of the low-angle bicrystals as a function of the misorientation angle obeys the Read–Shockley behavior and importantly, the obtained GB energies and structures are the same as obtained by Wojdyr et al. [6], who used a different variation of the Tersoff parameters [23]. To examine the mechanical response of the bicrystals, two representative GBs are investigated, a low-angle Σ365/(4.24°) and a high-angle Σ25/(16.26°). As seen in Fig. 2(a), the low-angle GB (Σ365) can be characterized as an array of edge dislocations. For these edge dislocation cores, the stable slip system was shown to be {110}⟨110⟩ [6]. In contrast, the high-angle GB (Σ25) can be characterized by periodic 6-membered rings (see Fig. 2(b)).

In order to examine the shear response of the systems under study, periodic boundary conditions were removed perpendicular to the GB, and the respective edges of the simulation cell were sheared by prescribing a fixed velocity of 0.1 Å/ps (10 m/s) to a rigid region of atoms located at one of the ends while keeping the other end fixed. This strain-rate corresponds to shock-loading scenarios; however, we found that at lower strain-rates (i.e., 0.01 Å/ps) no change in the characteristic mechanical response occurred.

Prior to application of shear strain, the systems were annealed at the desired temperature and at zero pressure using a Nose-Hoover thermostat and a Berendsen barostat, respectively. The temperatures at which the systems were examined equal 300 K, 900 K and 1800 K, in order to compare and contrast athermally and thermally driven phenomena. To ensure repeatability, a series of three simulations with different initial velocity distribution was

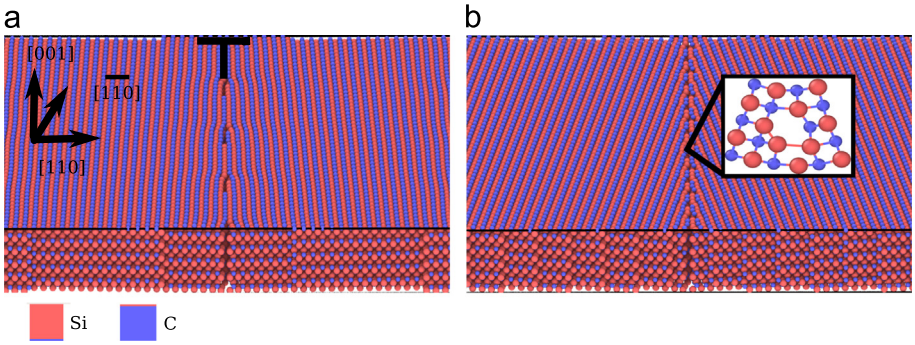

Fig. 2. Energy-minimum configurations of (a) low-angle (Σ365) and (b) high-angle (Σ25) GB. In the low-angle, the GB is characterized by dislocation array with $(\bar{1}10)[\bar{1}10]$ slip system and in high-angle, periodic 6-membered rings (shown in (b) inset).

performed; we note that the observed phenomenological behavior remained unchanged.

4. Results and discussion

Fig. 3 illustrates the shear-stress vs. displacement plot for both bicrystals at the different temperatures. At 300 K, as seen in Fig. 3(a), the mechanical response of the low-angle GB is characterized by an elastic regime followed by stick-slip behavior corresponding to the periodic 'saw-tooth' pattern in the stress vs. displacement curve. This observation is particularly interesting as stick-slip has not been reported for 3C-SiC or any material, which exhibits pure covalent bonding characteristics. The characteristic period (~3.15 Å) associated with stick-slip is a result of athermal shear-induced dislocation climb parallel to the GB. Specifically, this 'slide-climb' dislocation motion is found to occur by athermal climb characterized by piece-wise displacement of segments of the dislocation plane, as observed in the MD simulations (schematically shown in Fig. 3(c)). Interestingly, the ratio of shear modulus to the shear stress corresponding to the initiation of the stick-slip behavior (~4–5) is found to be similar to the theoretically predicted value of athermal climb of pure edge dislocations [27] In addition, the stick-slip behavior was found to be insensitive to the shear-velocity at which the grains were displaced with respect to each other. To emphasize this observation, we have included the shear stress vs. displacement response corresponding to a shear velocity of 0.05 Å/ps for the low-angle GB at 300 K.

To further characterize the stick-slip behavior in the 3C-SiC low-angle GB bicrystal, the spatial variation in the atomic shear strain corresponding to the initiation and completion of an underlying dislocation slide-climb (or equivalently the period of a saw-tooth in the resultant stress vs. displacement curve) is presented in Fig. 4. Here, the atomic local shear invariant strain is calculated using the Green-Lagrangian strain tensor defined as $\varepsilon = 1/2(F^T F - I)$, where F is the atomic deformation gradient tensor [22], which is defined with respect to the initial atomic configurations prior to shear application. Fig. 4(a) and (b) points to the fact that strain is concentrated at the GBs; importantly, the significant increase in the strain-concentration at the GB, as shown in Fig. 4b, is a result of the concerted slide-climb of the periodic dislocation cores.

With increasing temperature, distinct differences in the stress–strain response as well as the GB dynamics of the low-angle GB bicrystal can be observed (Fig. 3a). At 900 K, the stick-slip behavior is dampened and is characterized by an increase in period between peaks. Notably, dislocation glide along the $(\bar{1}10)[\bar{1}10]$ slip-system is observed in conjunction with athermal slide-climb of the dislocation cores along the GB. The fact that dislocation glide is thermally activated at 900 K while not at 300 K, clearly suggests that competing dislocation glide and athermal dislocation slide-climb mechanisms lead to dampened stick-slip at 900 K. The propagation of edge dislocations at 900 K along the slip plane is illustrated in terms of spatial maps of atomic shear strain before and after a stick-slip event as shown in Fig. 4(c and d). Similarly, nucleation and glide of dislocations in metallic materials for CSL-generated bicrystals has been previously observed although at lower temperatures [28]. At 1800 K, the low-angle GB bicrystal demonstrates little to no stick-slip under shear; the absence of stick-slip at 1800 K is a direct consequence of the interplay between thermal and shear induced effects leading to structural disorder in the GB as evidenced by the formation and increase in the number of homopolar C–C bonds at the GB with increasing shear deformation (Fig. 5a). The increased structural disorder and the resultant loss in the periodicity of the dislocation array within the GB, as a result of increased C–C homopolar bonds, leads to frictional drag behavior rather than stick-slip in response to the applied shear in a fashion similar to sliding of twist GBs in irradiated 3C-SiC [17]. In contrast to the high temperature behavior, as shown in Fig. 5(a), the shear induced structural disorder at the GB is minimal at lower temperatures and consequently the stick-slip is more pronounced especially at 300 K. Interestingly, the presence of chemical disordering has also been observed in irradiation studies of 3C-SiC GBs [16]. Additionally, studies of nano-polycrystalline SiC have shown an interplay between crystallization and chemical disordering of GBs at significant indentation depths [14]

An examination of the shear-stress vs. displacement curves for the high-angle GB bicrystal (Fig. 3(b)) shows that stick-slip behavior is reduced at 300 K as compared to the low-angle GB bicrystal at 300 K. This is directly correlated to the increase in homopolar C–C bonds for the high-angle GB with increasing deformation once displacement has occurred (Fig. 5(b)). This behavior is similar to that of the low-angle GB at 1800 K. An inspection of the high-angle GB structure reveals that the six-membered rings that characterize the unstrained GB were progressively broken prior to the formation of the covalent C–C bonds and as a result the majority of the broken rings did not re-form with increasing strain. An increase in temperature to 900 K leads to further chemical disordering as well as a reduction in stick-slip and at 1800 K, even the unstrained high-angle GB structure is sufficiently disordered which is consistent with earlier studies showing a monotonic increase in chemical disorder as a function of misorientation angle [16]. Consequently, deformation of the high-angle GB bicrystal is primarily due to frictional drag at the GB in response to the applied shear. To further illustrate the atomic disordering we use the common neighbor analysis [29] to determine the structural evolution of the GB region; here atoms with structural environments that deviate from the pristine diamond-cubic structure of 3C-SiC are colored light blue as shown in Fig. 6. In particular, the underlying atomic structures of the GB region for Σ365 and Σ25 are shown at 300 K and 1800 K before and after the

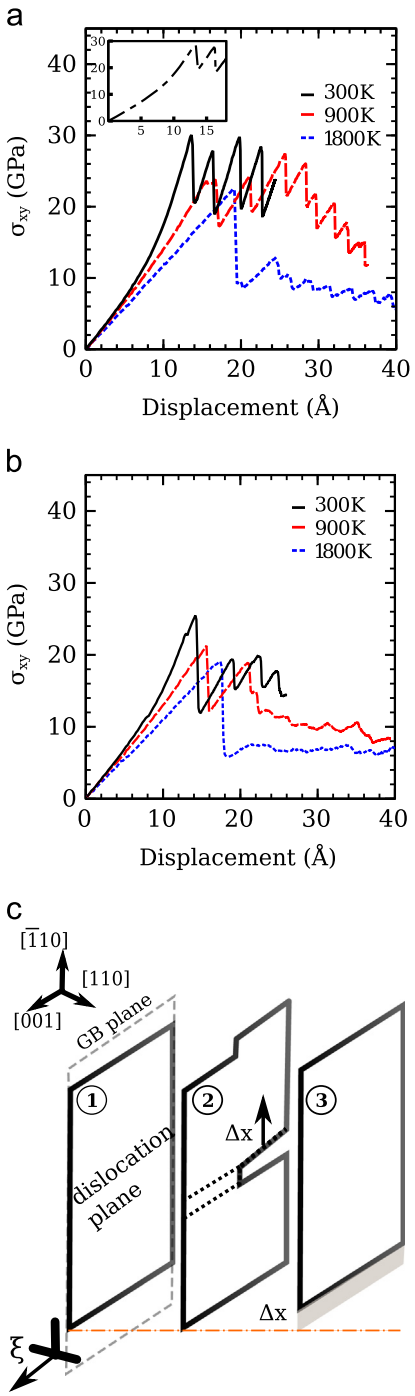

Fig. 3. Shear stress vs. shear displacement curves for: (a) low-angle (Σ365) (b) high-angle (Σ25) as a function of temperature at a shear velocity equal to 0.1 Å/ps. In (a) characteristic stick-slip behavior is seen at low-temperatures and progressively diminishes as temperature is increased. The inset in (a) represents the shear stress vs. displacement profile for a shear velocity equal to 0.05 Å/ps and a comparison shows that the stick-slip behavior is independent of the shear velocity. In (b) the chemical disordering reduces stick-slip even at 300 K for the high angle GB bicrystal. In (c) the piece-wise athermal climb characteristic of the low-angle grain boundary is shown as a sequence given by 1, 2, and 3 markers. Here ξ is the dislocation line sense and Δx the climb displacement.

respective simulations were completed. At 1800 K, both Σ365 and Σ25 demonstrate similar topological characteristics; at the lower temperature the final configurations of the respective systems differ significantly, with the low-angle GB retaining characteristic structural features even after the application of shear.

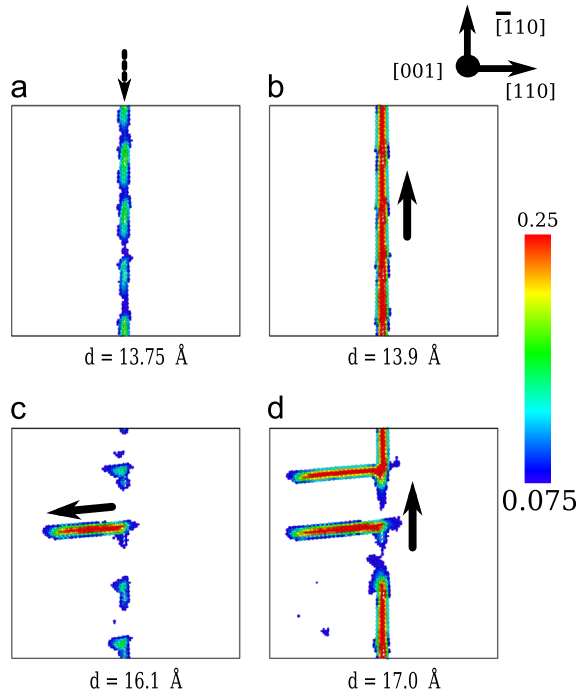

Fig. 4. Atomic shear strain maps as a function of shear displacement for the low-angle grain boundary bicrystal at 300 K ((a), (b)) and at 900 K ((c), (d)). Only atoms with strains above a threshold are shown and they are color coded based on atomic shear strain. At 300 K, the dislocation cores move parallel to the GB; the displacement has a magnitude of ~3.15 Å. In the 900 K simulation dislocation glide is activated along the $(\bar{1}10)[\bar{1}10]$ and dislocation movement parallel to GB also occurs. (For interpretation of the references to colour in this figure legend, the reader is referred to the web version of this article.)

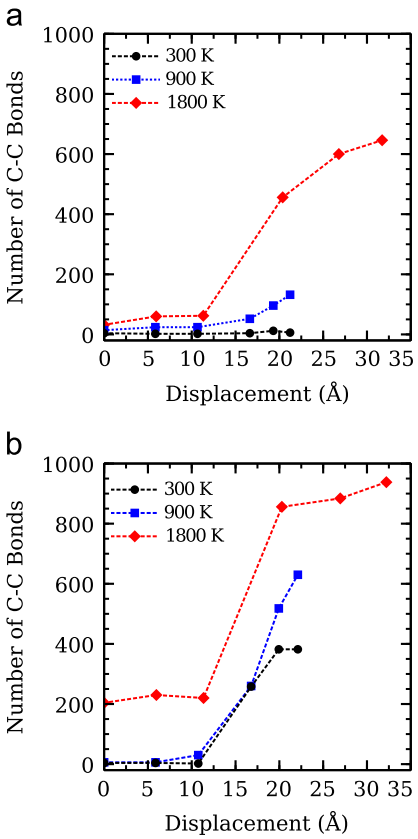

Fig. 5. Variation in C–C homopolar bonds at the GB as a function of shear: (a) low-angle and (b) high-angle at 300 K, 900 K, and 1800 K.

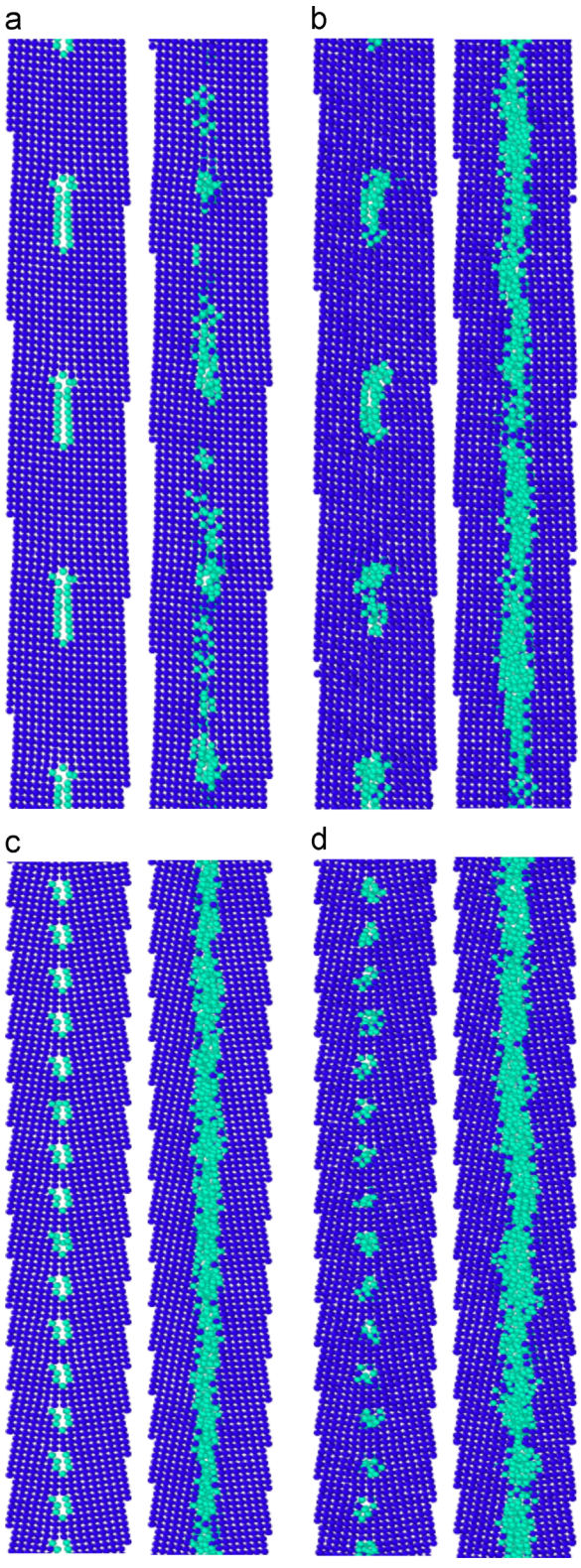

Fig. 6. Initial and final atomic configuration after shear loading of (a and b) Σ365 at 300 K and 1800 K, respectively, and (c and d) Σ25 at 300 K and 1800 K. Atoms are colored based on common neighbor analysis method. The light blue atoms deviate from pristine SiC diamond cubic structure indicating structural disordering. (For interpretation of the references to colour in this figure legend, the reader is referred to the web version of this article.)

Finally, in the context of this study it is worthwhile examining investigations of stick-slip in high-angle bicrystals of metallic systems such as copper in order to understand the salient aspects of GB dynamics of 3C-SiC under shear. In the metallic systems stick-slip was simultaneously accompanied by lateral GB migration and an underlying rearrangement of the constituent structural units in the GB [8,9]. The fact that we do not observe this coupling behavior for the low-angle (Σ365) 3C-SiC GB can be attributed to the low geometric coupling factor (0.07) as compared to the much higher coupling factor for the high-angle GBs examined in copper (0.67). Furthermore, for the high-angle Σ25 3C-SiC GB, while the coupling factor is higher (0.29), the lack of GB migration can be ascribed to the onset of structural disorder as discussed above. Here, the coupling factor (β) is defined by $\beta = 2\tan(\theta/2)$, where θ is the misorientation angle [7].

5. Conclusion

In conclusion, it is seen that the mechanical response of 3C-SiC bicrystals under shear is predominantly driven by the underlying GB structural characteristics. Thermal effects play a significant role in controlling the shear response of the bicrystals. The low-angle (Σ365) shear response can be classified into three temperature dependent regimes: at low-temperatures, shear deformation occurs via stick-slip which is attributed to the athermal slide-climb of dislocation cores in the GB plane; at higher temperatures dislocation glide along identified slip-planes are thermally activated leading to competing glide and slide-climb of dislocations and a consequent dampening of stick-slip. At higher temperatures, the GB becomes structurally disordered with increasing shear strain, which impacts the ensuing stick-slip shear response. In contrast, the high-angle GB bicrystal displays an increase in structural disorder at the GB relative to the low-angle GB at all temperatures, thereby exhibiting a considerably diminished stick-slip response.

The fundamental insights obtained from this work on the atomic-scale mechanisms that govern the mechanical response of 3C-SiC bicrystals represent an important step toward understanding and thus tailoring the microstructure of 3C-SiC for targeted technological applications where the ability to retain structural integrity at extreme conditions is paramount.

Acknowledgment

The author S.B. gratefully acknowledges the Thomas G. Chapman Fellowship awarded by the College of Engineering at the University of Arizona.

References

[1] M.A. Capano, R.J. Trew, MRS Bull. 22 (1997) 19.
[2] I. Szlufarska, K.T. Ramesh, D.H. Warner, Annu. Rev. Mater. Res. 43 (2013) 131.
[3] H. Kikuchi, R.K. Kalia, A. Nakano, P. Vashishta, P.S. Branicio, F. Shimojo, J. Appl. Phys. 98 (2005) 103524.
[4] Y. Mo, I. Szlufarska, Appl. Phys. Lett. 90 (2007) 181926.
[5] N. Swaminathan, P.J. Kamenski, D. Morgan, I. Szlufarska, Acta Mater. 58 (2010) 2843.
[6] M. Wojdyr, S. Khalil, Y. Liu, I. Szlufarska, Model. Simul. Mater. Sci. Eng. 18 (2010) 075009.
[7] J.W. Cahn, J.E. Taylor, Acta Mater. 52 (2004) 4887.
[8] J.W. Cahn, Y. Mishin, A. Suzuki, Acta Mater. 54 (2006) 4953.
[9] Y. Mishin, A. Suzuki, B.P. Uberuaga, A.F. Voter, Phys. Rev. B 75 (2007) 224101.
[10] J. Chen, L. Ouyang, W.Y. Ching, Acta Mater. 53 (2005) 4111.
[11] C.A.J. Fisher, H. Matsubara, Comput. Mater. Sci. 14 (1999) 177.
[12] H. Yoshida, K. Yokoyama, N. Shibata, Y. Ikuhara, T. Sakuma, Acta Mater. 52 (2004) 2349.
[13] K. Matsunaga, H. Nishimura, H. Muto, T. Yamamoto, Y. Ikuhara, Appl. Phys. Lett. 82 (2003) 1179.
[14] I. Szlufarska, A. Nakano, P. Vashishta, Science 309 (2005) 911.
[15] V.I. Ivashchenko, P.E.A. Turchi, V.I. Shevchenko, Phys. Rev. B 75 (2007) 085209.
[16] N. Swaminathan, M. Wojdyr, D.D. Morgan, I. Szlufarska, J. Appl. Phys. 111 (2012) 054918.

[17] E. Jin, L.-S. Niu, E. Lin, X. Song, J. Appl. Phys. 111 (2012) 104322.
[18] M. Kohyama, Phys. Rev. B 65 (2002) 184107.
[19] K. Muralidharan, K.-D. Oh, P.A. Deymier, K. Runge, J.H. Simmons, J. Mater. Sci. 42 (2007) 4159.
[20] M.J. Buehler, Atomistic Modeling of Materials Failure, Springer Science & Business Media, 2008.
[21] S. Plimpton, J. Comput. Phys. 117 (1995) 1.
[22] A. Stukowski, Model. Simul. Mater. Sci. Eng. 18 (2010) 015012.
[23] J. Tersoff, Phys. Rev. B 39 (1989) 5566.
[24] J. Tersoff, Phys. Rev. B 49 (1994) 16349.
[25] Z.G. Wang, J.B. Li, F. Gao, W.J. Weber, Acta Mater.. 58 (2010) 1963.
[26] C. Kohler, Phys. Status Solidi B 234 (2002) 522.
[27] U. Messerschmidt, Dislocation Dynamics During Plastic Deformation, Springer, Berlin Heidelberg, 2010.
[28] D.E. Spearot, K.I. Jacob, D.L. McDowell, Int. J. Plast. 23 (2007) 143.
[29] G.J. Ackland, A.P. Jones, Phys. Rev. B 73 (2006) 054104.